View metadata, citation and similar papers at core.ac.uk
brought to you by CORE
provided by idUS. Depósito de Investigación Universidad de Sevilla

Fischer–Tropsch synthesis in microchannels

L.C. Almeida (a), F.J. Echave (a), O. Sanz (a), M.A. Centeno (b), G. Arzamendi (c), L.M. Gandía (c), E.F. Sousa-Aguiar (d), J.A. Odriozola (b), M. Montes (a)

a Dept. Appl. Chemistry, University of the Basque Country, San Sebastian, Spain

b Inst. of Material Sciences of Seville, CSIC, University of Seville, Seville, Spain

c Dept. Appl. Chemistry, Public University of Navarre, Pamplona, Spain

d CENPES-PETROBRAS, Rio de Janeiro, Brazil

Abstract

Different metallic supports (aluminum foams of 40 ppi, honeycomb monolith and micromonolith of 350 and 1180 cpsi, respectively) have been loaded with a 20%Co–0.5%Re/γ-Al2O3 catalyst by the washcoating method. Layers of different thicknesses have been deposited onto the metallic supports. The catalytic coatings were characterized measuring their textural properties, adhesion and morphology. These structured catalysts have been tested in the Fischer–Tropsch synthesis (FTS) and compared with a microchannel block presenting perpendicular channels for reaction and cooling. The selectivity depends on the type of support used and mainly on the thickness of the layer deposited. In general, the C5+ selectivity decreased at increasing CO conversion for all of the systems (powder, monoliths, foams and microchannels block). On the other hand, the selectivity to methane increased with the thickness of the catalytic layer due to the higher effective H2/CO ratio over the active sites resulting from the higher diffusivity of H2 compared with CO in the liquid products filling the pores. The C5+ selectivity of the microchannels reactor is higher than that of the structured supports and the powder catalyst.

Keywords

Microchannels reactor; Structured supports; Washcoating; Fischer–Tropsch (FTS); Microreactors

1. Introduction

The FTS is a well-known catalytic process for the conversion of synthesis gas into liquid fuels. The main product of the process is a mixture of hydrocarbons of variable molecular weight. The reaction mechanism follows a polymerization-like scheme based on sequential –CH2– additions, that can be described with the Anderson–Schultz–Flory (ASF) product distribution, characterized by the chain growth probability parameter (α) [1]. This parameter, α, and consequently the selectivity significantly depend on the temperature because the activation energy of the termination step is higher than that of the growing step [2], [3] and [4]. Thus, high temperatures favor the formation of light products, mainly methane.

Taking into account the exothermal character of the FTS, the reactor design to obtain a good selectivity to middle distillates is predominantly guided by the temperature control.

Conventional packed-bed and slurry reactors have been used for the FTS. In the case of the packed-bed reactors, the internal mass-transfer limitations can be diminished using small catalyst particles or egg-shell pellets with thin catalytic layer. However, the pressure drop may become prohibitive if too small particles are selected. Furthermore, the use of conventional packed-bed reactors is limited by heat removal [5], making necessary to use diluted catalyst beds. In contrast, slurry reactors can work with very small catalyst particles, which prevent internal diffusional limitations; moreover, the well-mixed reaction mixture results in nearly isothermal operation that allows running the process at higher CO conversion per pass. However, catalyst particles for these reactors have to be optimized to resist to mechanical stress and attrition and an efficient filtrating system has to be developed for the liquid products/catalyst separation [1].

One of the main advantages of using metallic substrates like monoliths to prepare structured catalysts, is the possibility of applying a thin layer of catalyst with controlled thickness in a fixed body of a large-scale reactor with very low pressure-drop [6]. Thin catalyst layers may prevent diffusion limitations. The tuneability of the catalytic layer thickness allows designing the monolithic catalyst for optimal activity and selectivity [7]. Other important advantages of the use of washcoated monoliths are the high gas–liquid mass transfer rates in two-phase flow, the possibility of using high liquid and gas throughputs, and the fact that no separation between liquid products and the catalyst is necessary [1].

In FTS, carbon monoxide and hydrogen have to be transported from the bulk gas phase to the active sites inside the catalyst pores. Not only is the catalyst effectiveness an important factor but the selectivity of the reaction is also very much dependent on the presence of both reactants in about stoichiometric amounts. The effective H2/CO local ratio changes from the outside of the catalyst particle toward the inside because of the higher hydrogen diffusivity in the liquid products filling the pores. Large diffusion lengths lead to the depletion of carbon monoxide. These local super-stoichiometric amounts of hydrogen result in lower chain-growth probabilities and, therefore, lighter products [8]. Therefore, the relation between diffusion limitations and selectivity is complex. Both the reactants (gases) and the reaction products (gases and liquids including waxes) play an important role. It is clear that diffusion limitations play a crucial role in the activity and selectivity of Fischer–Tropsch synthesis catalysts. On the other hand, the FTS is significantly exothermic, so it is necessary to remove the heat to avoid hot-spots in the catalysts, resulting in the formation of light hydrocarbons. Several secondary reactions of 1-olefins influencing the overall selectivity of the FTS have been described: (i) isomerisation to internal olefins, (ii) cracking and hydrogenolysis, (iii) hydrogenation to paraffins, and (iv) chain ionization [9]. Intraporous diffusional resistance favors olefins readsorption, the first step of all these reactions, and changes the actual H2/CO ratio over the active sites, modifying their relative importance and consequently the overall FTS selectivity. The decrease in the olefin to paraffin ratio has been related to the increase in the internal mass-transfer limitations [1]

Hilmen et al. [7] investigated the FT activity of different monolithic systems in a comparative study using catalysts with similar composition. It was shown that high washcoat loadings

resulted in lower C5+ selectivities and olefin/paraffin ratios due to the increased transport limitations. On the other hand, Kapteijn et al. [10] reported an extensive and systematic study on the effect of the catalytic layer thickness (20–110 µm) on the FTS in cordierite monoliths. They showed that washcoat layers thicker than about 50 µm led to internal diffusion limitations.

In this paper an experimental investigation on structured catalysts for FTS using metallic supports of different geometries is reported. The investigated structures include aluminum foams, honeycomb monoliths with different cpsi and a microchannels reactor. The catalytic performance of the supported catalyst was assessed, in terms of both activity and selectivity comparing supports with the same catalytic load per volume unit. Catalytic tests with the catalyst in powder form were also carried out for comparison.

2. Experimental

2.1. Catalyst preparation

A powder catalyst containing 20 wt.% cobalt and 0.5 wt.% rhenium was prepared by one-step incipient wetness co-impregnation of γ-Al2O3 support (Spheralite SC505, Procatalyse) with an aqueous solution of cobalt nitrate hexahydrate and perrhenic acid. The support and aqueous metal solution were mixed under ambient temperature and pressure conditions. Before impregnation, the support (<60 µm) was calcined in a muffle at 773 K for 10 h with a heating rate of 1 K/min. After impregnation, the catalyst was dried at 393 K for 3 h and finally calcined at 623 K for 10 h at a heating rate of 2 K/min.

2.2. Structured catalyst supports

2.2.1. Supports pre-treatment and forming

Several types of structured supports were used: parallel channel monoliths, foams and a microchannels block. Homemade parallel channel monoliths consisting of 50 µm Fecralloy sheets (Goodfellow) corrugated using rollers producing different channel sizes were fabricated. Monoliths were made by rolling around a spindle alternate flat and corrugated sheets. DUOCEL aluminum foam from ERG Materials and Aerospace of 40 ppi was used (void fraction 0.927; geometric surface area 235 m2/m3). Foams were cut out from slabs using a hollow drill with a diamond saw border. Both monoliths and foams were cylindrical (D = 16 mm; L = 30 mm). The microchannels (depth: 700 µm; width: 700 µm; length: 20 mm; number of channels per plate: 10) were fabricated on Fecralloy (Goodfellow) by microdrilling. The machined plates were joined together placing metallic sheets (Fe79/B16/2 Goodfellow) between them and further were diffusion bonded. The final block was composed of 100 microchannels for reaction in 10 plates welded intercalated by 10 additional plates presenting 100 microchannels for cooling in cross flow arrangement. The geometric characteristics of the investigated structured supports are compiled in Table 1.

In order to improve the interaction between the washcoat layer and the metallic support, the surface of both monolith and foam was modified. The monoliths and micromonoliths were pretreated in air for 22 h at 1173 K to generate α-alumina whiskers (see Fig. 1A). Aluminum

foams were pretreated by anodization in 1.6 M oxalic acid at 323 K, 40 min and 2A/foam for obtaining a rough alumina surface (see Fig. 1B) [11].

2.2.2. Preparation of the slurry

The washcoating method was used to cover the structured substrate with the slurries prepared from previously synthesized catalysts. Preparing stable slurries of the catalyst to be deposited is the first step to washcoat a metallic substrate. The catalyst was ball milled for 5 h to obtain small particles. The particle size (d4,3) after ball milling was 3.4 µm. To obtain stable slurries of different solids, particle size distributions below 10 µm are recommended [12]. The catalyst content of the suspension was kept constant at 20 wt.% (beyond this value their viscosity increased significantly). Nyacol AL20 colloidal alumina (C.A.) and poly vinyl alcohol (PVOH) were used as additives. The viscosity of the prepared slurry was 10.5 mPa s at shear rate of 3240 s^{-1}. The pH of the catalyst slurry was adjusted employing diluted HNO3. The isoelectric point (IEP) of the catalyst is around 9 and therefore a pH 4 will ensure high values of zeta potential and then high repulsions between the particles, which favors the stability of the slurries [13].

2.2.3. Washcoating

The structured supports were dipped into the slurry for 60 s, withdrawn at constant speed of 3 cm min^{-1} and then, the suspension excess was eliminated by centrifugation at 500 rpm for 5 min for the monoliths and foam and air blowing for the plates and microchannels block. The coating was repeated several times using the same slurry with a drying step at 393 K for 30 min between coatings to deposit 250, 500 and 1000 mg of the catalyst. Finally, coated structured supports were calcined at 623 K for 6 h.

To washcoat the microchannel block, it was previously covered with masking tape to protect the entire exterior surface except the entry and exit of the microchannels to be coated. Afterwards, it was carried out the coating of the catalyst using the same procedure and slurry as for the structured supports. Then, elimination of the excess was made by the blowing technique.

2.3. Characterization

Particle size distribution of the catalyst was measured with a laser particle size analyzer (MALVERN MasterSizer 2000). One hundred milligrams of solid were dispersed in 20 mL H2O and the pH adjusted to 4, promptly submitted to ultrasounds for 1 h before the measurement.

The Zeta Potential was measured using a MALVERN Zetasizer 2000 instrument. The solids were dispersed in an aqueous solution of 0.003 M NaCl. The pHs of the solutions were adjusted with HNO3 or NaOH solutions.

Rheological properties of the slurries were measured in a rotational viscosimeter HAAKE, model VT 500, geometry NV.

The adherence of the catalytic layer deposited onto the substrates was evaluated using an ultrasonic technique. The weight loss caused by the exposition of the sample to ultrasounds is measured. The structured supports immersed in petroleum ether were submitted to an ultrasonic treatment for 30 min at room temperature. After that, the samples were dried and calcined. The weight loss was determined by the difference in the mass of the samples before and after the ultrasonic test. The results are presented in terms of the retained amount of coating on the monolith, expressed as percentage.

The catalyst coating morphology was studied by optic microscopy (Leica Microscope M165C + DFC 420) and scanning electron microscopy (SEM) Hitachi S-2700.

Textural properties of the structured supports and powder catalyst were determined by nitrogen adsorption using a Micromeritics ASAP 2020. A homemade cell that allows analyzing the complete structured supports was employed. Average thickness layer was calculated as $\delta = WS{-}1D{-}1$, where W is the amount of catalyst loaded, S the geometrical surface of the monolith of foam, and D the density of the coating. D is estimated as 0.825 g/cm3 using the specific gravity of alumina, the pore volume of the alumina particles measured by nitrogen adsorption and the void fraction between the catalyst particles in the coating (0.45).

2.4. Catalytic tests

The FTS was carried out in a commercial Computerized Microactivity Reference Catalytic Reactor from PID Eng&Tech, employing a Hastelloy C-276 tubular reactor (Autoclave Engineers) with an internal diameter of 17 mm. Prior to reaction the catalyst was reduced at 623 K during 10 h in a stream of pure H2 with a total flow of 120 ml/min gcat. The experimental runs were conducted with a H2/CO molar ratio in the feed of 2. The total flow rate was varied for powders, foams and monoliths between 45 and 180 mL/min that resulted in space velocities between 4785 and 26886 mL/min gcat. Fro the microchannel block, the catalyst load (164 mg) and the flow rate used (8.2–6 mL/min) produced space velocities between 3000 and 24,146 mL/min gcat. A trap at 120 °C before the pressure regulation valve retained the high molecular products (waxes). Gaseous products were taken out through a thermostatic line at 473 K and analyzed with a 6890 Agilent GC, using a FID for C5 to C18 hydrocarbons and a TCD to analyze H2, CO, CO2, N2, H2O, CH4 and light hydrocarbons until C4.

FTS in the microchannel block was also performed in the hot box of the Microactivity apparatus (PID Eng & Tech) using the same feeding and analysis lines. The temperature control was carried out with and auxiliary pressurized water line passing throughout the microchannels perpendicular to the reaction ones. This cooling concept was previously checked by computational fluid dynamics simulations [14].

3. Results

3.1. Optimization of the slurry properties and washcoating process

Stable slurries (non-settling) are obtained when the terminal velocity of the particles is very small. Small velocities are the result of compensating the gravity force by the drag force. Particle settling is well-known in the creeping flow regime that states for Newtonian fluids in

which, the terminal velocity depends directly on the square of the particle size and the difference in density between the solid and the fluid, and inversely on the fluid dynamic viscosity. Therefore, for a particular solid and liquid (usually water) to increase the stability is convenient to reduce the particle size and to increase the viscosity of the medium. In this regard, a study of the catalyst milling (Retsch ball mill S100, agate mortar 250 mL, 10 agate balls of 2 mm) was carried out. The particle size practically did not change after 5 h of grinding (see Fig. 2A). The initial particle size distribution of the catalyst and that after 5 h milling presenting an average particle size (d4,3) of 3.4 µm are compared in Fig. 2B.

Another important parameter in the preparation of a stable slurry is the zeta potential of the solid. This variable indicates the pH range suitable to maximize the repulsion between particles and consequently, to improve the slurry stability. The evolution of the zeta potential in function of the pH for the solid considered in this study is shown in Fig. 3. It can be seen that the isoelectric point of the solid is around 8.8 and the values of zeta potential are relatively large (+40 mV) at pH below 7.

The key parameter that controls the washcoating process is viscosity. Low viscosities allow obtaining highly adherent and homogeneous structures but with low specific loads. Thus, for obtaining the target loading, several coatings are required. On the contrary, high viscosity will allow high specific load per coating although the homogeneity is lower (accumulations and risk of channels blocking) resulting in less adherence of the coating. The optimal viscosity usually ranges between 5 and 30 mPa s (at 3200 s^{-1}) as proposed by several authors [15], [16], [17] and [18]. The colloidal alumina additive presents a narrow particle size distribution [15] improving the catalyst adherence. Nijhuis et al. [16] proposed a model in which the smaller particles are located between the bigger ones increasing the adherence. On the other hand, the PVOH additive improved principally the drying process of washcoating.

Several trials of slurry formulation for washcoating on the structured supports (not shown here) were carried out and the characteristics (specific load, homogeneity and adhesion) of the resulting coatings examined. Finally, the following composition of the slurry was selected: 20% catalyst content, 1% PVOH (w/w), 5% C.A. (w/w) and pH of the suspension adjusted to 4 with HNO3.

Regarding the washcoating process, a strategy of increasing complexity passing form monoliths to single microchannels plates and finally to the complete microchannels block was followed. The first step was to study the coating of the catalyst over the structured supports (monoliths and foam). Once this objective was achieved and knowing the fundamental aspects of the coating of these systems, the next step was coating plates with removable cover allowing to observe the coating inside the microchannels. Then, welded plates were coated and finally, the selected recipe and procedure was used to coat the microchannels block.

3.2. Preparation of the structured catalysts

3.2.1. Monoliths and foam

The washcoating method was chosen to deposit the catalyst onto the structured supports due to its simplicity and versatility. A series of structured substrates, monoliths (M), µmonoliths (µM) and foams (F) with different loadings of the catalyst (20%Co-0.5%Re/γ-Al2O3) was prepared. The goal was to load the structured substrates with 250, 500 and 1000 mg of the solid. Different aliquots of the same parent slurry were used for repeated coatings. Table 2 shows the properties of the coating (load, number of coating and adherence) and the textural properties of the structured and powder catalyst, for both the fresh sample and that obtained after drying and calcination of the slurry.

In Fig. 4, the amount of catalyst loaded over the substrates is plotted versus the number of coatings. It is shown that the specific load increases almost linearly with the number of coatings. The washcoating method gives additive and homogeneous results. In addition, it can be observed that the foam presents a higher specific load than the monoliths. This result could be related to the data of geometrical surface area used to calculate the specific load. This value is difficult to measure for foams and has been obtained from the information brochures of the manufacturer. The discrepancy observed in Fig. 4 suggests that, in absence of other factors influencing the results, the geometrical surface of the foam could be overestimated by about 100%.

It can be seen from Table 2 that adhesion is slightly higher in micromonoliths than in monoliths and significantly higher than in the foams. Furthermore, increasing the load decreased the adhesion. This is clearer in the monoliths and foams than in micromonoliths. These results could be related to the different geometrical surface areas of the three substrates used and consequently to the different coating thicknesses. Indeed, as can be seen in Table 1, by passing from foams to monoliths and micromonoliths, the geometrical surface area increases, and for the same global load (250, 500 and 1000 mg), the thickness (see Table 3) decreased significantly. So, it is also important to remark the significant geometric differences between monoliths and foams. In the case of monoliths, the coating is inside the channels and their concave form helps the adhesion blocking mechanically the coating inside the channels (see Fig. 5A–D). The same reasoning would also explain the higher adhesion of the micromonoliths compared to the monoliths. In contrast, the coating on foams is external to the struts making more difficult its adhesion (Fig. 5E). Additionally, due to the low geometrical surface area of foams very thick coatings are required to reach the same global loading. As a result, some material is retained partially blocking the macropores of heavily loaded foams (Fig. 5F).

The specific surface area of the coating was measured by nitrogen adsorption and compared to that of the powders (parent catalyst and dried and calcined slurry). It can be seen from the data in Table 2 that the specific surface area of the coating decreases slightly with respect to that of the parent catalyst, but the same occurs for the powder obtained after drying and calcination. Therefore, this decrease in surface area could be related to the additional thermal treatment during drying and calcination. Although the texture of the coated foams was studied, no surface area of the coating could be calculated because the anodized foams presented a high surface area that varied during the coating process making impossible to obtain the value of the coating with enough accuracy [19].

3.2.2. Microchannel plates and microchannel block

Two types of microchannels plates were used: with removable cover using nuts and bolts (µP) and welded (µPW). Firstly, microchannel plates were recovered with masking tape (that is easily removed after the process of washcoating). The catalyst was deposited into the microchannel plates using the washcoating technique and the same suspension employed with the monoliths and foams. The excess was eliminated by air blowing and subsequently the plate was dried at 333 K. At the end of each coating, the adhesive tape was removed to weight the amount of catalyst loaded. Finally, the plates were calcined for 6 h at 623 K. The µP were used to check the adhesion of the coating and the µPW to observe the homogeneity of the coating within the channels. The same technique was used to coat the microchannels block (µCB). Fig. 4 shows the specific load (mg/cm2) increase as a function of the number of coatings for both types of plates and for the microchannels block. The loading increase is in all cases additive and linear. Fig. 6 shows SEM micrographs of the plates and microchannels block. Fig. 6 A is a general view of the catalytic coating on the microchannels plate, showing that the coating inside the microchannels is homogeneous and free of cracks. Fig. 6B–D shows different views of the catalytic layer coated in the microchannels confirming the homogeneity of the coating.

4. Discussion

4.1. Fischer–Tropsch synthesis (FTS)

The performance in the FTS of the structured catalysts (monolith, micromonoliths and foam), microchannels block, parent catalyst and the powder obtained from the slurry is compiled in Table 3. The powder from the slurry was sieved in the range lower than 60 µm and between 60 and 100 µm. All the experiments were carried out keeping the H2/CO ratio = 2 and a total pressure of 10 bar. It was studied the influence of the temperature and the space time (varying the amount of the catalyst loaded on the structured substrate or the feed flow rate). Table 3 shows that in this series of experiments the conversion of CO varied between 8.3% and 81.5%, and the selectivity to methane between 16.2% and 28% when using the structured catalysts, which is coherent with the relatively high temperature considered (523 K) in most of the cases. In general, it was observed that the selectivity to olefins was significantly higher for the structured support than for the powder catalyst, independently of the CO conversion or the catalyst layer thickness. As reported by Visconti et al. for similar structured catalyst [1], this is an evidence of the lower diffusional limitations produced by the structured supports. Powder catalysts gave low values of the selectivity to C5+, especially when the catalyst was not diluted in the packed bed. As selectivity to C5+ decreases at increasing temperature, the better performance of the structured catalyst suggests a better temperature control that in diluted powder catalysts, and this one better than the undiluted bed.

In what follows the activity and selectivity results will be discussed in three separate sections considering the effects of the coating thickness, the FTS temperature and feed flow rate, respectively. In all cases, a general trend can be observed: as the CO conversion increases, the selectivity to C5+ decreases. Similar results have been recently reported by Marion and Hugues using a Co catalyst and working at high CO conversions [20]. This could be explained by the different diffusivities of H2 and CO and the influence of the water–gas shift (WGS) reaction. Indeed, increasing the CO conversion produces more flow in both directions (reactants and products) throughout the liquid filling the catalyst pores, increasing the resistance to the

diffusion of the reactants leading to an increase in the effective H2/CO ratio on the catalytic sites due to the higher diffusivity of H2[21]. Consequently, the production of light hydrocarbons is favored. On the other hand, increasing the CO conversion increases the production of water. Recently, Marion and Hugues have reported that with Co catalyst in FTS at high Co conversion values the water produced favored the WGS reaction producing additional hydrogen and consuming CO, that also increased the ratio H2/CO and the selectivity to CH4 and CO2[20].

4.2. Influence of the catalyst layer thickness (δ)

Monoliths, micromonoliths and foams have been loaded with different amounts of catalyst and then different layer thicknesses (see Table 3). As shown in Fig. 7 the structured catalysts present a higher selectivity to C5+ than the powder catalyst in spite of the dilution of the bed used to improve the temperature control [22]. These results could be related with the high exothermicity of the FTS reaction. The diffusion of the reactants and products and the heat removal are influenced by the multiphase flow regime in the catalytic beds. Liu et al. [17] have suggested that the capillarity forces not only retain liquid in the pores, but also between the particles of the powder catalyst forming aggregates and preferential paths in packed beds reactors. This is in contrast with the structured reactors where the catalytic layer is covered by a thin film of liquid that makes easier the mass and heat transport. It can be seen also that the C5+ selectivity for the structured catalysts decreases in the following order: micromonoliths > foams > monoliths. At low CO conversions, foams present the same C5+ selectivity than the micromonoliths, in spite of the catalytic layer thickness in the foams, which is three times higher than in the micromonoliths. This good performance of foams could be related with the more mixed flow (more turbulent) prevailing in this substrate compared to the perfect laminar flow in the monoliths channels. Nevertheless, at high CO conversions, a change in the C5+ selectivity of the foams can be observed as a result of the excessive loading (see Fig. 5F), cancelling the positive effect of the flow regime. On the other hand, comparing monoliths and micromonoliths (almost the same flow regime), Fig. 7 shows that the C5+ selectivity in monoliths is lower than in micromonoliths, in accordance with the fact that the thickness of the catalytic layer at the same catalyst loading is higher for the monoliths.

4.3. Influence of the temperature

The influence of the reaction temperature has been studied using the structured catalysts M500-2, µM500-2 and E500-2, as can be seen in Table 3. The temperature has been varied between 493 and 523 K at syngas flow of 90 mL/min. The apparent activation energy can be calculated using the rates of CO consumption obtained from the catalytic tests at the several temperatures [10]. Using data in Table 3, the apparent activation energy values calculated were 104, 100.8 and 90.8 kJ/mol, for the monoliths, foams and micromonoliths, respectively. These values are slightly lower to that reported by Kapteijn et al. [10] 115 kJ/mol.

Fig. 8 shows that the evolution of the selectivity to C5+ depends on both the reaction temperature and the CO conversion. An increase of the temperature increases the differences between the performances of the structured systems. Increasing the temperature, increases the CO conversion and as discussed before, the selectivity to lighter hydrocarbons. Moreover, as the activation energy of the termination step is higher than that of the growing step,

increasing temperature also favors the selectivity to light products even at constant CO conversion. When moving from foams to monoliths and micromonoliths, the geometrical area of the metallic substrate increases, then, for the same amount of catalyst, the thickness of the catalytic layer decreases. As a consequence, there is a lower diffusion resistance and better temperature control, enhancing the C5+ selectivity in the order: micromonoliths > monoliths > foams.

4.4. Influence of residence time

Monoliths and microchannels block have been tested in the FTS varying the syngas flow between 8.2 and 66.0 mL/min in the case of the microchannels block and between 30 and 180 mL/min in the case of the monoliths. The pressure has been maintained at 10 bar and temperature at 523 K. Fig. 9 shows the variation of the C5+ selectivity versus the CO conversion for the structured supports and for the microchannels block. Decreasing the space velocity (decreasing flow rate), increases the CO conversion and decreases the C5+ selectivity in the following order: microchannels block > micromonoliths > monoliths. There is an influence of the catalytic layer thickness on the C5+ selectivity as discussed before: the higher thickness the lower C5+ selectivity. But this relationship does not apply for the microchannel block that presents high layer thickness (35.5 µm) and the highest selectivity to C5+. Therefore, it seems that the effective temperature control achieved with the microchannels block offsets the negative effect of the layer thickness.

5. Conclusions

The viability of the use of structured supports for the Fischer–Tropsch synthesis has been evidenced in this study. Information about the key parameters of the design and fabrication of supported catalysts and microchannels block has been given. The results show that the supported catalysts and the microchannels block present better performance than the powder catalyst. In addition, the selectivity to C5+ depends on the type of support and mainly on the amount of catalyst deposited and its effect on the catalytic layer thickness. On one hand, it has been observed that the C5+ selectivity decreases with the increase in the CO conversion, which could be explained by the higher diffusivity of H2 in the pores filled with the liquid products and by the effects of the WGS reaction on the effective H2/CO ratio.

The C5+ selectivity decreases for the structured systems in the following order: microchannels block > micromonoliths > monoliths > foams. This can be related to the catalytic layer thickness in the case of the structured supports, and to the better temperature control in the case of the microchannels block. Therefore, controlling the coating process (specific load and geometry) and microreactor configuration are key parameters for a good microreactor design for the Fischer–Tropsch synthesis.

Acknowledgements

Financial support by PETROBRAS, the Spanish MICINN (MAT2006-12386-C05 and ENE2009-14522-C05) and UPV/EHU (GIU07/63) are gratefully acknowledged. TEKNIKER is acknowledged for the mechanical construction.

References

[1] C.G. Visconti, E. Tronconi, L. Lietti, G. Groppi, P. Forzatti, C. Cristiani, R. Zenanaro, S. Rossoni

An experimental investigation of Fischer–Tropsch synthesis over washcoated metallic structured supports

Appl. Catal. A: Gen., 370 (2009), pp. 93–101

[2] K.R. Krishna, A.T. Bell

Estimates of the rate coefficients for chain initiation, propagation, and termination during Fischer–Tropsch synthesis over Ru/TiO2

J. Catal., 139 (1993), pp. 104–118

[3] M.E. Dry

The Fischer–Tropsch process: 1950–2000

Catal. Today, 71 (2002), pp. 227–241

[4] H. Schulz

Short history and present trends of Fischer–Tropsch synthesis

Appl. Catal. A: Gen., 186 (1999), pp. 3–12

[5] C. Perego, R. Bortolo, R. Zennaro

Gas to liquids technologies for natural gas reserves valorization: the Eni experience

Catal. Today, 142 (2009), pp. 9–16

[6] F. Kapteijn, T.A. Nijhuis, J.J. Heiszwolf, J.A. Moulijn

New non-traditional multiphase catalytic reactors based on monolithic structures

Catal. Today, 66 (2001), pp. 133–144

[7] A.M. Hilmen, E. Bergene, O.A. Lindvag, D. Schanke, S. Eri, A. Holmen

Fischer–Tropsch synthesis on monolithic catalysts of different materials

Catal. Today, 69 (2001), pp. 227–232

[8] R.M. de Deugd, F. Kapteijn, J.A. Moulijn

Trends in Fischer–Tropsch reactor technology—opportunities for structured reactors

Top. Catal, 26 (2003), pp. 29–39

[9] C.H. Bartholomew, R.J. Farrauto

Fundamentals of Industrial Catalytic Processes

(2nd edition)Wiley-Interscience, Hoboken, NJ (2006) pp. 420

[10] F. Kapteijn, R.M. de Deugd, J.A. Moulijn

Fischer–Tropsch synthesis using monolithic catalysts

Catal. Today, 105 (2005), pp. 350–356

[11] O. Sanz, F.J. Echave, M. Sanchez, A. Monzon, M. Montes

Aluminium foams as structured supports for volatile organic compounds (VOCs) oxidation

Appl. Catal. A: Gen., 340 (2008), pp. 125–132

[12] J.R. Gonzalez-Velasco, M.A. Gutierrez-Ortiz, J.L. Marc, J.A. Botas, M.P. Gonzalez-Marcos, G. Blanchard

Pt/Ce0.68Zr0.32O2 washcoated monoliths for automotive emission control

Ind. Eng. Chem. Res., 42 (2003), pp. 311–317

[13] S. Vallar, D. Houivet, J. El Fallah, D. Kervadec, J.M. Haussonne

Oxide slurries stability and powders dispersion: optimization with zeta potential and rheological measurements

J. Eur. Ceram. Soc., 19 (1999), pp. 1017–1021

[14] G. Arzamendi, P.M. Diéguez, M. Montes, J.A. Odriozola, E. Falabella Sousa-Aguiar, L.M. Gandía

Computational fluid dynamics study of heat transfer in a microchannel reactor for low-temperature Fischer–Tropsch synthesis

Chem. Eng. J., 160 (2010), pp. 915–922

[15] L.C. Almeida, F.J. Echave, O. Sanz, M.A. Centeno, J.A. Odriozola, M. Montes

Washcoating of metallic monoliths and microchannel reactors

Stud. Surf. Sci. Catal., 175 (2010), pp. 25–33

[16] T.A. Nijhuis, A.E.W. Beers, T. Vergunst, I. Hoek, F. Kapteijn, J.A. Moulijn

Preparation of monolithic catalysts

Catal. Rev., 43 (2001), pp. 345–380

[17] D.J. Liu, D.R. Winstead, N. Van Den Bussche, Method of preparing a catalyst layer over a metallic surface of a recuperator, US Patent 6,540,843 B1 (2003).

[18] V. Meille, S. Pallier, G.V. Santacruz, C. Bustamante, M. Roumanie, J.P. Reymond

Deposition of gamma-Al2O3 layers on structured supports for the design of new catalytic reactors

Appl. Catal. A: Gen., 286 (2005), pp. 232–238

[19] R.C. Spooner, D.J. Forsyth

Aluminum, 46 (1970), pp. 165–169

[20] M.-C. Marion, F. Hugues

Modification of cobalt catalyst selectivity according to Fischer–Trospch process conditions

Stud. Surf. Sci. Catal., 167 (2007), pp. 91–96

[21] E. Iglesia, S.C. Reyes, R.J. Madon, S.L. Soled

Selectivity control and catalyst design in the Fischer–Tropsch synthesis: sites, pellets and reactors

Adv. Catal., 39 (1993), pp. 221–302

[22] R. Myrstad, S. Eri, P. Pfeifer, E. Rytter, A. Holmen

Fischer–Tropsch synthesis in a microstructured reactor

Catal. Today, 147 (2009), pp. S301–S304

Figure captions

Figure 1. SEM image of the monolith after pre-treatment: (A) Fecralloy and (B) aluminum

Figure 2. Effect of grinding time on particle size distribution for the Co–Re/γ-Al2O3 catalyst powder: (A) cumulative volume distribution versus grinding time and (B) volume distribution versus particle size.

Figure 3. Zeta potential of Co–Re/γ-Al2O3 particles in function of pH.

Figure 4. Specific load of the different structures as a function of the number coatings to reach the objective load. µP and µPW: plates of microchannels; µCB: microchannel block; F: foam; M: monolith; µM: micromonolith.

Figure 5. Optical image of for different structured supports washcoated with Co–Re/γ-Al2O3: (A) M500, (B) M1000, (C) µM500, (D) µM1000, (E) F500 and (F) F1000.

Figure 6. SEM micrograph of Co–Re/γ-Al2O3 catalyst deposited on plate and block microchannels.

Figure 7. Activity (CO conversion) and selectivity (C5+) for different catalyst layer thicknesses at 250 °C, 10 bar and H2/CO = 2.

Figure 8. Activity (CO conversion) and selectivity (C5+) at different temperatures, 10 bar, syngas flow 90 mL/min and H2/CO = 2.

Figure 9. Selectivity to C5+ versus CO conversion (different space velocities) of the monoliths, micromonoliths and microchannels block presenting different catalyst layer thicknesses at 200 °C, 10 bar and H2/CO = 2.

Table 1

Table 1. Geometric characteristics of the investigated structured supports.

Structured support	**Monolith**	**Micromonolith**	**Foam**	**Microchannels block**
				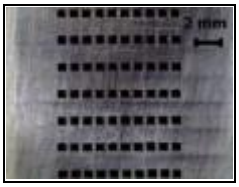
Geometric surf. (cm^2)	258	510	140	56
Hydraulic diameter (μm)	835	373	700	700
Porosity (%)	89	79	95	–
ppi (pores/in.^{2})	–	–	40	–
cpi (cells/in.^{2})	350	1180	–	–
Dimension				
∅ (mm)	16	16	16	–
L (mm)	30	30	25	20

Table 2

Table 2. Washcoating characteristics of the prepared structured catalysts.

Catalyst		**Washcoating**			**Textural property**		
		Load (mg)	**Number of coatings**	**Adhesion (%)**	S_{BET} **(m^2/g_{cat})**	V_{Pores} **(cm^3/g)**	D_{Pore} **(nm)**
Monolith	M250	255.3	5	93.8	–	–	–
	M500	490.4	11	92.6	160	0.28	5.4
	M1000	908.3	27	81.3	–	–	–
μmonolith	μM250	271.7	3	96.2	–	–	–
	μM500	592.9	4	96.0	163	0.26	5.6
	μM1000	1081.0	14	94.4	–	–	–
Foam	E250	262.1	4	78.0	–	–	–
	E500	549.3	11	76.2	252	1.01	10.8
	E1000	907.5	20	63.2	–	–	–
Slurry powder	–	–	–	–	166	0.26	5.5
	–	–	–	–			
	–	–	–	–			
Powder catalyst		–	–	–	184	0.27	5.2

Table 3

Table 3. Performance in the FTS of the catalysts indicated (10 bar and H_2/CO molar ratio of 2).

Catalyst		**FTS conditions**			***δ* (μm)**[a]	**CO conversion and selectivity data**				
		***T* (°C)**	**Qsyngas (mL/min)**	**Wcat. (mg)**		**% CO**	**% CH_4**	**% C_{5+}**	**% CO_2**	**$C_3{=}$/C_{3-}**
Monolith	M250	250	90	255.3	12.4	19.2	20.8	64.3	0.18	1.780
	M500-1			490.4	23.8	42.0	24.2	58.8	0.88	0.772
	M1000			908.3	44.0	58.2	27.1	55.9	2.89	0.419
	M500-2	220	90	739.3	35.8	8.3	19.7	71.3	1.03	1.190
		235				19.3	22.1	63.0	1.21	1.000
		250				47.5	25.2	59.3	1.66	0.860
	M500-3	250	45	401.7	19.5	48.4	20.1	75.0	2.13	1.002
			90			35.1	19.5	76.7	1.65	1.604
			180			16.0	16.2	78.0	1.10	2.505
μmonolith	μM250	250	90	271.7	6.5	25.2	18.3	68.9	0.23	1.407
	μM500-1			379.6	9.0	35.6	20.9	65.7	0.71	1.067
	μM1000			1081.0	25.7	71.5	22.8	58.8	4.90	0.549
	μM500-2	220	90	592.9	14.1	14.2	16.6	73.8	1.54	1.260
		235				30.2	19.8	68.1	0.97	1.090
		250				59.7	23.2	63.4	1.41	0.910
	μM500-3	250	45	564.2	13.4	65.8	18.9	78.5	1.80	0.402
			90			50.4	20.2	76.8	1.20	0.504
			180			18.5	22.4	73.2	0.50	1.509
Foam	F250	250	90	262.1	22.7	23.4	17.5	70.8	0.20	1.507
	F500-1			549.3	47.6	53.9	26.0	57.8	2.00	0.550
	F1000			907.5	78.6	81.5	28.0	52.0	8.64	0.400
	F500-2	220	90	631.5	54.7	11.6	17.1	73.3	1.5	1.110
		235				23.8	20.9	59.7	2.1	0.900
		250				51.8	26.4	56.3	2.7	0.790
	F500-3	250	45	925.6	80.1	77.9	22.3	72.3	5.90	1.207
			90			64.8	20.1	75.7	5.45	1.408
			180			38.1	18.2	74.0	3.67	1.904
Channel block (20 bar)		220	8.2	164.0	35.5	50.5	17.9	76.5	0.55	0.305
			16.5			32.0	18.1	80.0	0.57	1.101
			33			10.0	10.2	86.5	0.87	1.202

Catalyst		FTS conditions			δ (µm)[a]	CO conversion and selectivity data				
		T (°C)	Qsyngas (mL/min)	Wcat. (mg)		% CO	% CH_4	% C_{5+}	% CO_2	$C_3^{=}/C_3^{-}$
			66			6.0	5.0	92.0	1.20	1.403
Slurry powder	<60 µm + SiC	250	90	252.0	10[b]	33.1	20.1	64.4	1.0	0.35
				500.0		45.3	26.5	56.6	3.6	0.34
				954.0		69.7	30.7	48.5	5.9	0.23
	60–100 (m + SiC	250	90	254.0	17[b]	35.8	21.5	60.5	1.6	0.34
				550.0		50.5	27.3	52.4	3.7	0.22
				951.0		73.5	31.3	47.8	6.9	0.22
Catalyst + SiC		250	90	456.0	10[b]	69.7	30.7	48.0	5.9	0.30
Catalyst		250	90	0.453	10[b]	90.0	85	5.0	8.1	0.12

a Average thickness layer calculated as $\delta = WS^{-1}D^{-1}$, where $D = 0.825$ g/cm^3 assuming spherical particles.

b $D = 1/6$ dp, assuming spherical particle.

Figure 1

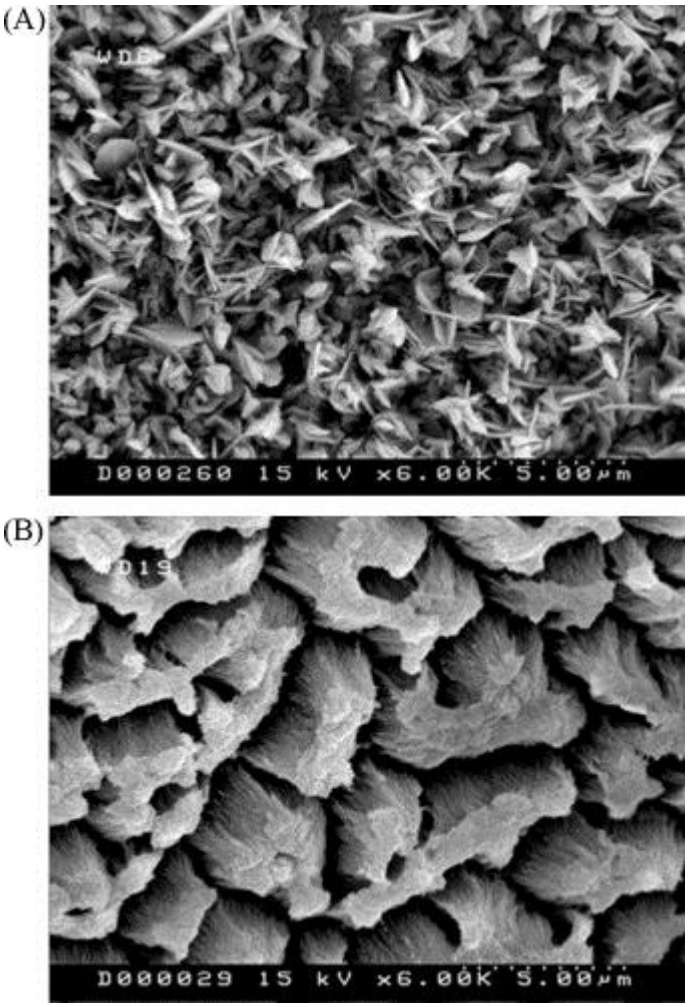

Figure 2

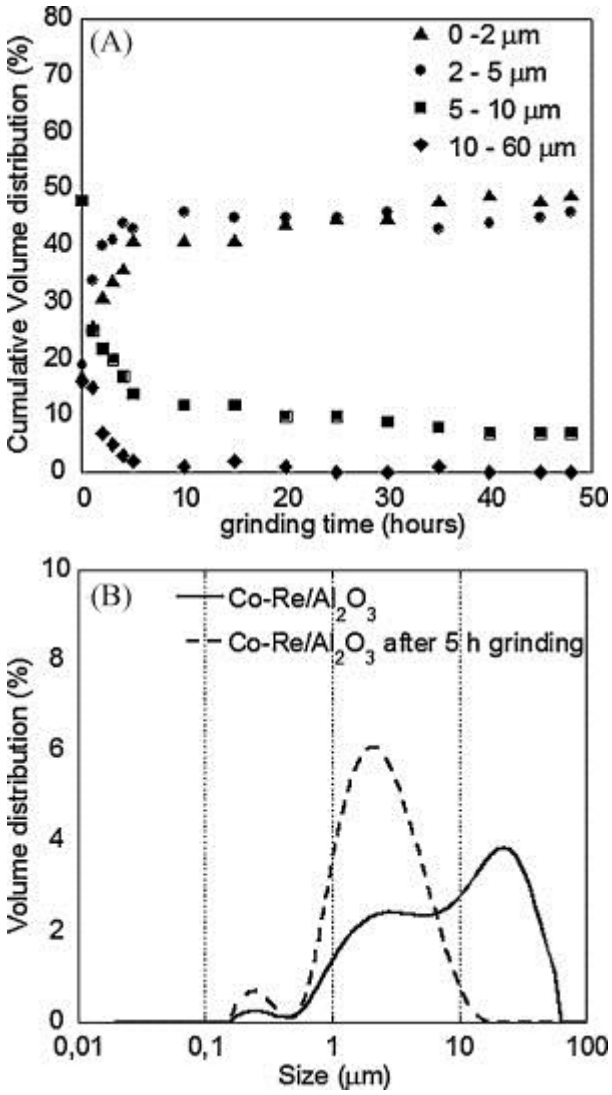
(A)
0 -2 μm
2 - 5 μm
5 - 10 μm
10 - 60 μm
Cumulative Volume distribution (%)
grinding time (hours)
(B)
Co-Re/Al2O3
Co-Re/Al2O3 after 5 h grinding
Volume distribution (%)
Size (μm)

Figure 3

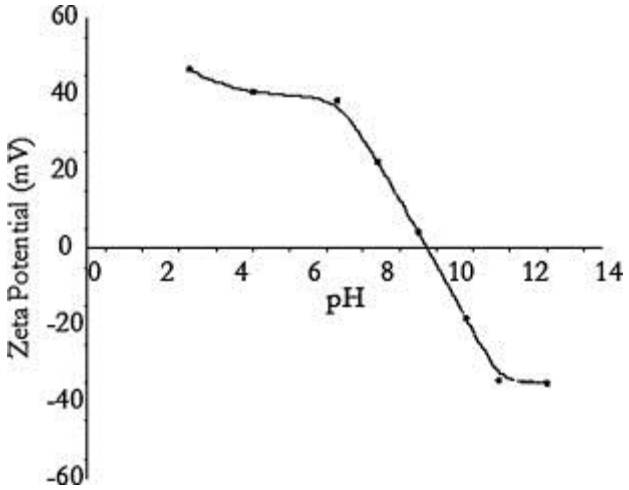

Figure 4

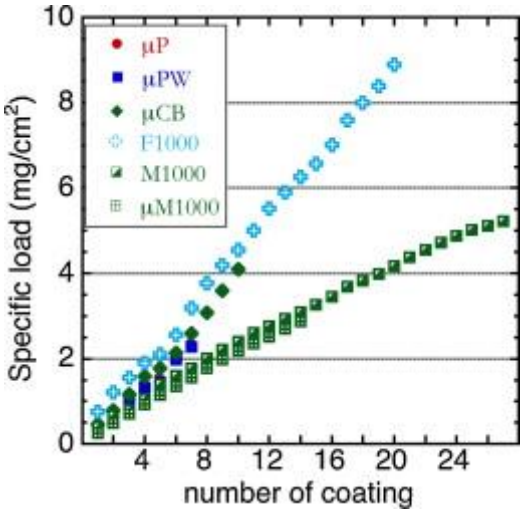
μP
μPW
μCB
F1000
M1000
μM1000
Specific load (mg/cm²)
number of coating
0
2
4
6
8
10
4
8
12
16
20
24

Figure 5

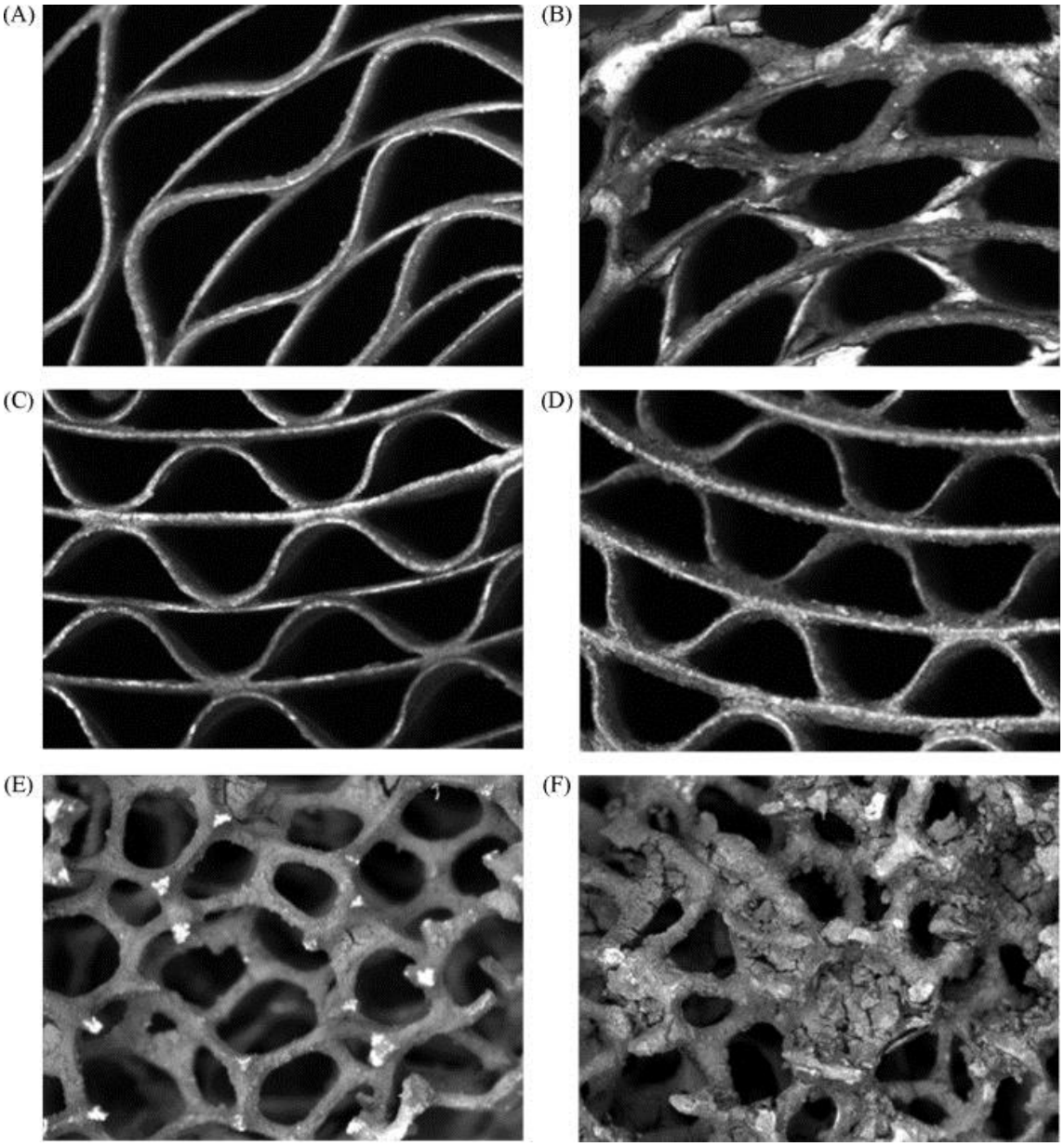

Figure 6

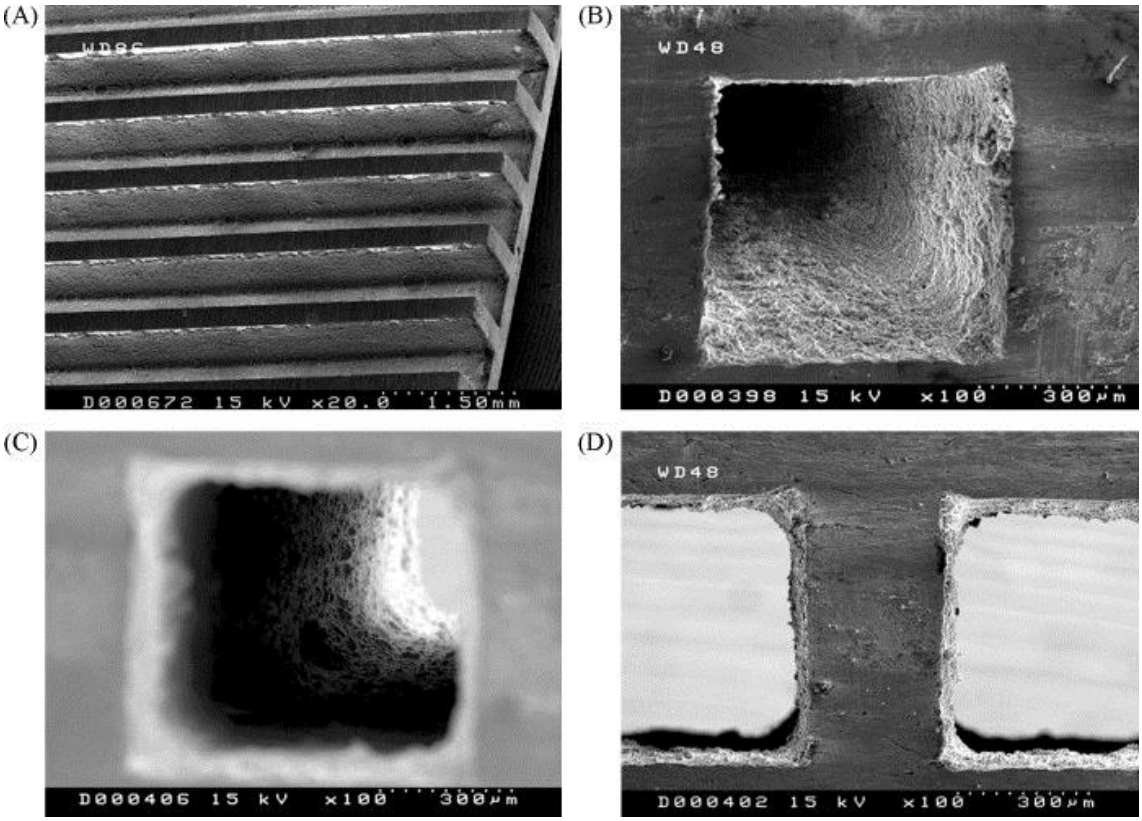
(A)
WD8S
D000672 15 kV x20.0 1.50mm
(B)
WD48
D000398 15 kV x100 300µm
(C)
D000406 15 kV x100 300µm
(D)
WD48
D000402 15 kV x100 300µm

Figure 7

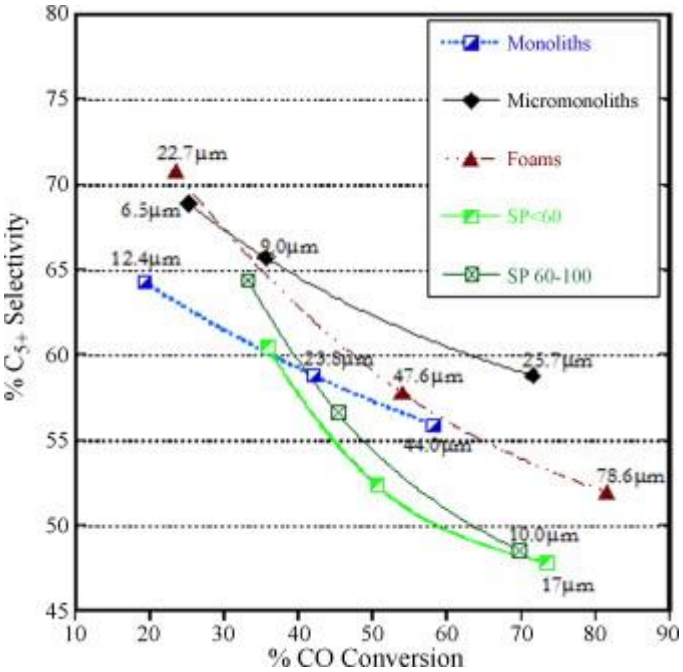
Monoliths
Micromonoliths
Foams
SP<60
SP 60-100
22.7µm
6.5µm
12.4µm
9.0µm
23.8µm
47.6µm
25.7µm
44.0µm
78.6µm
10.0µm
17µm
% C_{5+} Selectivity
% CO Conversion
80
75
70
65
60
55
50
45
10
20
30
40
50
60
70
80
90

Figure 8

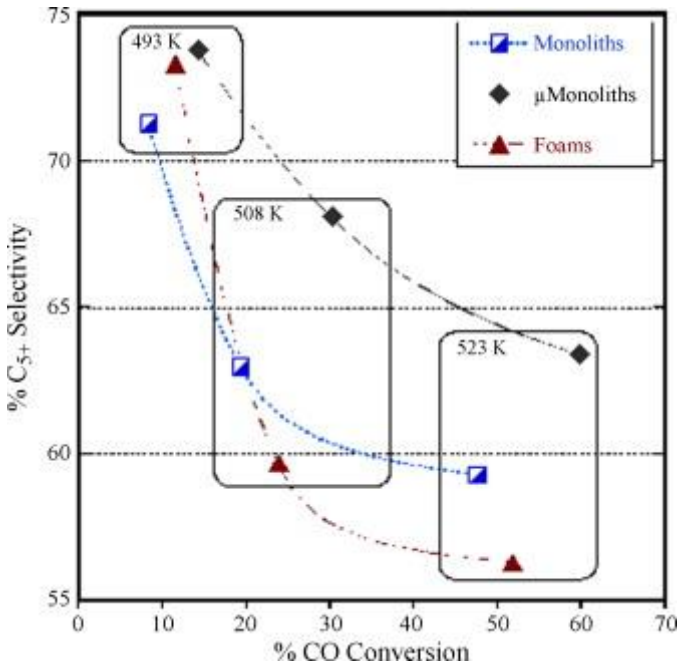
493 K
508 K
523 K
Monoliths
µMonoliths
Foams
% C_{5+} Selectivity
% CO Conversion
75
70
65
60
55
0
10
20
30
40
50
60
70

Figure 9

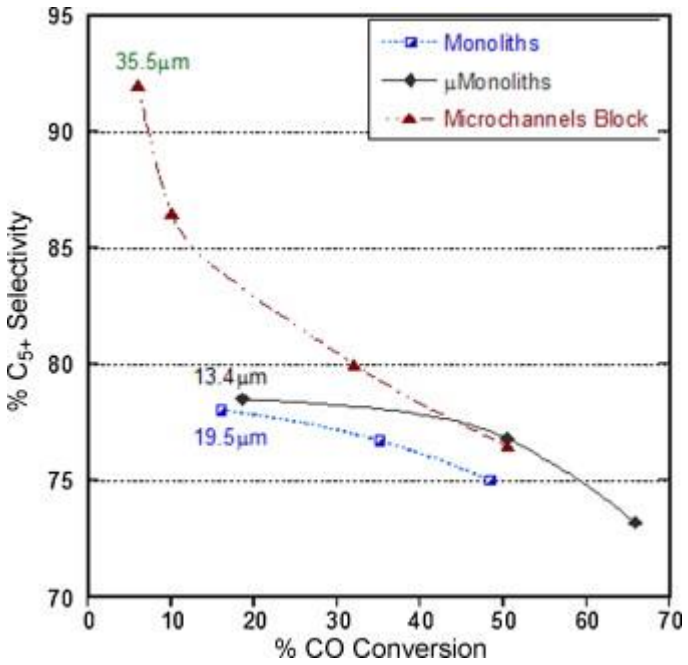
Monoliths
µMonoliths
Microchannels Block
35.5µm
13.4µm
19.5µm
% C5+ Selectivity
% CO Conversion
95
90
85
80
75
70
0
10
20
30
40
50
60
70